Dynamic Temporal Decorrelation: An Information-Theoretic and Biophysical Model of the Functional Role of Lateral Geniculate Nucleus

Wilson A. Truccolo and Dawei W. Dong

Center for Complex Systems and Brain Sciences
Florida Atlantic University
Boca Raton, Florida 33431

Email: truccolo@walt.ccs.fau.edu dawei@dove.ccs.fau.edu

(*Neurocomputing* Vol 38-40, page 993-1001, 2001)

Abstract

We investigate if well-known LGN ion channel properties can facilitate information-theoretic optimal coding through temporal decorrelation; and if so, whether the degree of temporal decorrelation can be adapted dynamically to ensure such optimization at longer time scales. Significant temporal decorrelation for time lags above 50 ms is achievable in a LGN cell model with inputs generated from natural visual stimuli. Dynamic decorrelation is obtainable through adaptive temporal filtering by varying the resting membrane potential. We conclude that the biophysical properties of LGN cells support the role of temporal decorrelation and enable a plausible feedback control mechanism that dynamically adapt to changes in input statistics.

1 Introduction

Until recent years, the lateral geniculate nucleus (LGN) was commonly assumed a relay station between retina and visual cortex, through which no significant transformation of visual information happens beyond simple gain control (LGN cells fire less number of spikes than its retinal inputs). However, if one examines the temporal aspects of retinal and LGN cell responses, there are some important differences for a wide range of operating conditions. The response of the LGN cells is much more transient than the retinal ganglion cells; the LGN cells also perform a sharper temporal bandpass filtering of the incoming signal [6, 7]. LGN cells can fire in two distinct modes of activity: tonic and bursting spikes, and it has been shown that both types of spikes can carry visual information [4, 11]. Furthermore, recent evidence shows that the temporal properties of the LGN response vary continuously with the degree of bursting present in the spike train, making the extreme tonic/burst dichotomy obsolete. In this way, LGN cells can work as tunable temporal filters, where the tuning is given by modulatory control of the cells' membrane resting potential and consequently the conductances and kinetics of the T-type Ca^{2+} channels [10, 8]. The modulatory control could come from the nonretinal input to the LGN. It is known that retinal terminals represents only $\sim 10 - 20$ % of synaptic inputs onto LGN. The nonretinal input derives from descending corticogeniculate axons, local feedback circuits, and ascending axons from the brainstem reticular formation. It was suggested that the nonretinal input plays the role of a gain control which gates the information flow through the LGN [14, 1, 5, 13].

We suggest that LGN can play an important role in the optimal coding of sensory information in time — optimal from an information-theoretic point of view. Since under natural viewing conditions, the visual signal sent to the LGN is temporally redundant or inefficient, LGN can do a lots more than simple gain control. It has been proposed earlier [2] that LGN is concerned with improving efficiency of visual representation through temporal decorrelation. The present study investigates if the well-known LGN ion channel properties, especially the T-type Ca^{2+} current, can facilitate such information-theoretic optimal coding; and if so, whether the degree of temporal decorrelation can be adapted dynamically to ensure such optimization at longer time scales. Three aspects are addressed: how the temporal decorrelation is achieved, how fast the decorrelation mode is activated, and how efficient the LGN's coding is under different modulatory states.

2 Methods

2.1 The LGN cell model

We model the type of LGN cells which receive direct inputs from retina and send output to visual cortex. The LGN cell model incorporates the quantitative kinetics of the Ca^{2+} channel and the Hodgkin-Huxley K^+ and Na^+ channels of active membrane currents. The membrane potential V_m changes according to

$$\frac{\mathrm{d}V_m}{\mathrm{d}t} = -(I_{N_a} + I_K + I_T + I_{leak} + I_{EPSP})/C_n \tag{1}$$

in which I_{N_a}, I_K, and I_T are the Na^+, K^+, and Ca^{2+} currents, respectively. C_n is the membrane capacitance. All the channel properties are well known [9] and the parameters are similar to a previous model [10]. The leak current is given by

$$I_{leak} = G_{leak}(V_m - V_r) \tag{2}$$

in which the leak conductance G_{leak} is taken as a constant. The leakage reversal potential V_r is the only parameter controllable according to a simple measure of autocorrelation of the cell's output, and it is used to achieve dynamic temporal decorrelation. The retinal input to LGN is modeled by the monosynaptic current I_{EPSP} generated by the input spike train according to an alpha function. When the LGN cell has no retinal input, its resting membrane potential will be close but not equal to the leakage reversal potential V_r. The effects of nonretinal input are reflected by different V_r values.

2.2 Input spike trains to LGN

The model LGN neuron is simulated with input stimuli generated from real-world time-varying light intensities recorded by a moving camera [3]. The digitized light intensity values around the center pixel were used to generate time series that were then pre-processed to mimic the retinal ganglion cell responses (spatial filtering at different scales, corresponding to different sizes of receptive fields). The resulting signal was used to modulate the firing rate of non-homogeneous Poisson spikes that generated the input spike trains to the LGN. The light intensity time series were separated in two main groups with different degree of temporal correlation in order to probe the model cell's responses. The first group (I1) has very long-lasting temporal correlations and was obtained by filtering through a large spatial receptive field, i.e., DOG filter at a low spatial frequency ($\sim$ 0.3 cycle/degree). The second one (I2)

has a very small temporal correlation and was obtained by filtering through a small spatial receptive field, i.e., DOG filter at a high spatial frequency (~ 5 cycle/degree). (For more details of the dependence of the temporal correlations on spatial scales, see [3].) Additional pre-processing by mimicking the effect of temporal filtering at the retina level almost completely decorrelated the time series from the second group but introduced no significant temporal correlation change in the first group (for the references on retina filtering, see [2]).

2.3 Tonic and bursting spikes

Hyperpolarization, achieved by controlling V_r, results in an overall reduction of the number of LGN output spikes. This is expected since lowering V_r will lower the gain and/or threshold of the LGN cell in response to its input. But it is not a simple gain control.

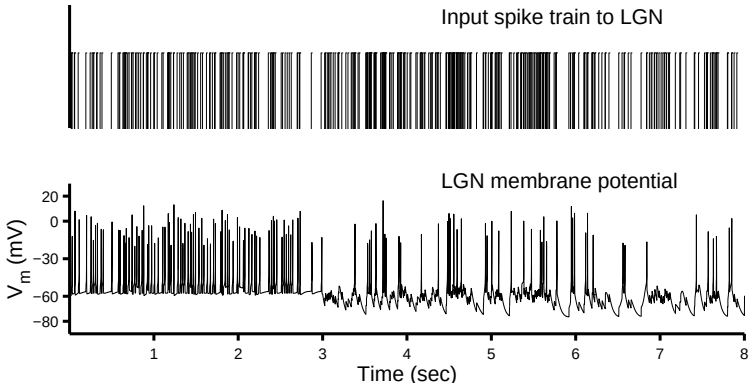

Figure 1: Transition from tonic to burst spikes. Top pannel: input spike train to LGN. Bottom pannel: LGN's output spike train. At time $t = 3$ seconds the leakage reversal potential V_r is changed from -60 to -80 mV. The activation of the calcium dynamics is fast (~ 100 ms) such that the cell can produce bursts very shortly after the transition.

More interestingly (Figure 1), the hyperpolarization activates the Ca^{2+} channel with a time constant of $\sim$ 100 ms. Such activation generates bursting spikes in addition to tonic spikes, resulting in temporal differentiation on the Ca^{2+} channel time scale. When $V_r = -60$ mV, the cell fires tonic spikes, which almost replicate the input spikes except missing one or two occasionally; when $V_r = -80$ mV, the cell fires burst spikes, which are a lots less frequent than the input and concentrated roughly at where the input changes. We want to know how V_r affects the overall temporal encoding in LGN in a quantitative manner.

3 Results

3.1 How temporal decorrelation can be achieved

We use the autocorrelation function $C(\tau)$ to measure the temporal correlation of the binned and mean-subtracted spike train $S(t)$:

$$C(\tau) = \frac{< S(t+\tau)S(t) >_t}{< S(t)S(t) >_t} \tag{3}$$

in which $<>_t$ denotes averaging over time t. It is obvious that the function $C(\tau)$ equals to 1 when the time lag $\tau = 0$. In all the plots shown in the following figure, a bin size of 50 ms is used for calculating $C(\tau)$. We have tried a bin size of 25 ms and similar results were obtained.

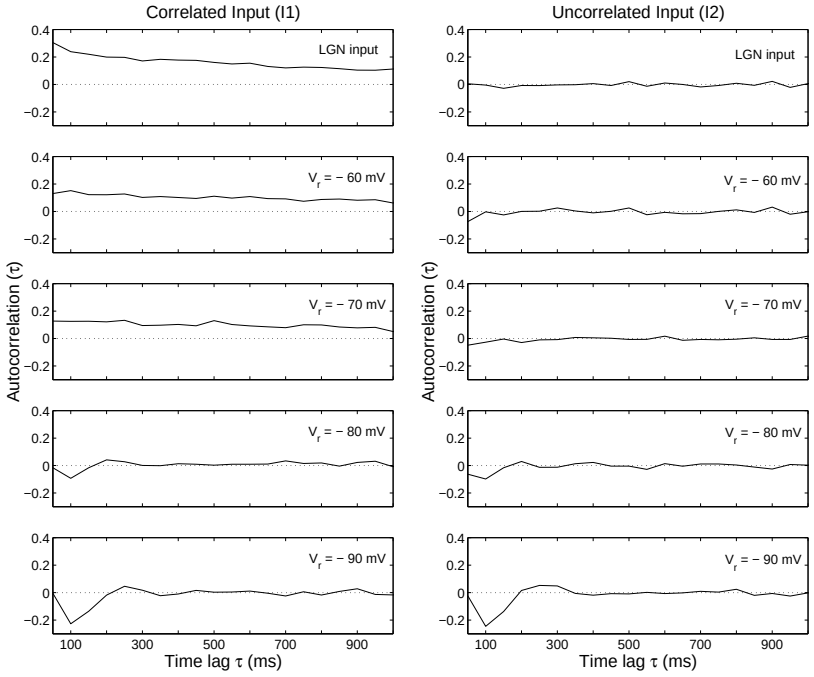

Figure 2: Decorrelation level dependence on leakage reversal potential. Left: the top panel shows the autocorrelation function of the input spike train to the LGN cell, the other 4 panels refer to the autocorrelation function of the LGN cell's spike train for different levels of the leakage reversal potential V_r; the highest decorrelation level is achieved at $V_r \sim -80$ mV. Right: the same as in the right panels, with the exception that here the input spike train had no temporal correlation and the output decorrelation is best achieved at $V_r \sim -60$ mV. The autocorrelation was computed over segments of 256 seconds.

The Figure 2 shows the simulation result on how temporal decorrelation depends on the leakage reversal potential V_r. Since the degree of correlation of the output is

always relative to the input, the results for the two input spike trains (I1 and I2) are shown, which simulate the changes of inputs statistics at a longer time scale. For all tested natural stimuli, significant temporal decorrelation for time lags above 50 ms is achievable through variable temporal filtering of the model by simply selecting a V_r between slight-depolarization to hyper-polarization for each stimulus; in the former case, the LGN cell relays uncorrelated input, and in the later case, decorrelates highly correlated signals. The necessary V_r for decorrelation has a monotonic relationship to the cross-correlation at the Ca^{2+} channel time scale, which enables a plausible feedback control on a longer time scale when input statistics change.

3.2 How fast the decorrelation mode is activated

To investigate how long it takes for the LGN cell model to switch from one mode to another, we started the simulation with V_r at -60 mV. At time equal to 3 seconds, V_r was set to -80 mV, such that the calcium dynamics is activated (Figure 1). It is clear that in the normal range of input I_{EPSP}, which has roughly 40 spikes per second, the cell is hyperpolarized soon after (within ~ 100 ms) and the calcium channel gets activated.

In this particular simulation, the input spike trains are generated from the highly correlated time series (I1). As expected from the previous section, the autocorrelation $C(\tau)$ before the switch ($V_r = -60$ mV) has significant correlations over a long period of time; and the autocorrelation $C(\tau)$ long after the switch ($V_r = -80$ mV) has no significant correlations, i.e., the LGN output is decorrelated. The question is how fast the decorrelation sets in.

To investigate that we need to calculate the time-dependent correlation function $C(t, \tau)$ to measure the temporal correlation of the binned and mean-subtracted spike train $S(t)$:

$$C(t, \tau) = \frac{< S(t + \tau)S(t) >_e}{< S(t)S(t) >_e} \tag{4}$$

in which $<>_e$ denotes ensemble averaging over many trials with different input spike trains (but the same statistics). Figure 3 shows the correlation function $C(t, \tau)$ before, near, and after the V_r switch. It is clear that the LGN cell starts decorrelating as soon as 150 ms after the transition. This means that the temporal decorrelation by hyperpolarization can play a role of dynamic gain control at ~ 100 ms time scale which not only change the gain of LGN cells but optimize its information content about the input.

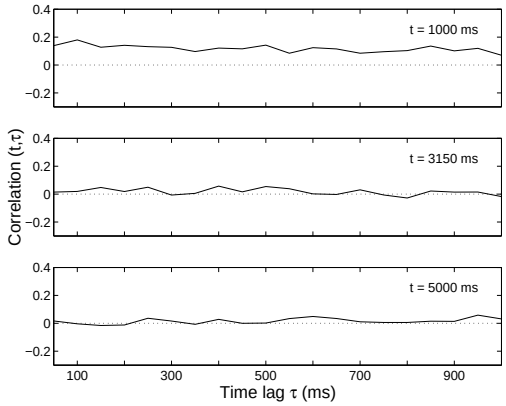

Figure 3: Transition to the decorrelation mode. The LGN cell is simulated for 8 seconds with the correlated input spike train I1. As in Figure 1, at time equal to 3 seconds, the leakage reversal potential V_r is changed from -60 mV to -80 mV to test how fast the cell enters the decorrelation mode. Top panel, V_r is at -60 mV and the LGN output spike train has temporal correlations. Middle panel, 150 ms after the change to $V_r = -80$ mV ($t = 3150$ ms), the LGN output spike train is already decorrelated. Bottom panel: 2 seconds after the change, the LGN cell keeps decorrelating the input spike train. The auto-correlation was computed from an ensemble of 620 trials of 8 seconds long, each from a different light intensity segment. A bin size of 50 ms is used for calculating $C(t, \tau)$.

3.3 How efficient the LGN's coding is

In this section we investigate how the coding efficiency of the LGN cell is affected in the two activity modes. Information measures are employed to address this issue [12]. The measures were computed according to the following formulas. The coding efficiency is measured by the mutual information M:

$$M = T - N \tag{5}$$

in which the total information T and the noise information N are

$$T = -\sum_W P(W)\log_2 P(W) \qquad N = -\left\langle \sum_W P(W|t)\log_2 P(W|t) \right\rangle_t \tag{6}$$

The $P(W)$ is the probability of the 10 bits word W obtained by digitizing the LGN output spike train with a bin width of 10 ms. A base 3 was used to discriminate from 0 to 2 spikes per bin. The input to LGN used for the computation of the total information consisted of two spike trains, each 2,200 seconds long, that were generated from two distinct (correlated or decorrelated) nonrepeated segments of natural image light intensity. For the computation of the noise information, the correlated input (I1) ensemble consisted of 400 realizations of nonhomogeneous poisson spikes,

each 64 seconds long, generated from a single 64 seconds segment of correlated light intensity. Similarly, the decorrelated input (I2) ensemble was generated from a 64 seconds segment of decorrelated light intensity. The $P(W|t)$ is the probability of the 10 bits word W at a given time t and $\langle\ \rangle_t$ denotes averaging over time.

Table 1: The total, mutual, and noise information of LGN output spike train for different inputs and at different leakage reversal potentials. The spike rate is given in spikes per second (Hz) and the information quantities is in bits per spike. The estimated error for the information is about 10^{-2} bits/spike.

	V_r (mV)	Spike Rate	Total	Noise	Mutual
I1	-60	24.60	3.10	2.65	0.45
	-80	6.47	5.80	4.80	1.00
I2	-60	24.90	3.10	2.71	0.39
	-80	6.66	5.22	4.92	0.30

The results are shown in Table 1. Overall the results indicate that a higher efficiency of coding can be achieved for the two types of visual inputs by setting the leakage reversal potential at different levels: for the input with long lasting temporal correlation (I1), setting V_r to -80 mV ensures that the corresponding LGN output is decorrelated and improves the efficiency of coding from 0.45 bits/spike to 1.00 bits/spike; for the input with little temporal correlation (I2), setting V_r to -60 mV ensures that the corresponding LGN output is decorrelated and improves the efficiency of coding from 0.30 bits/spike to 0.39 bits/spike. It is important to notice that the absolute information rate (bits per second) is always greater for $V_r = -60$ mV, especially because the firing rate of the cell for $V_r = -60$ mV is about 4 times higher than for $V_r = -80$ mV. In other words, while the decorrelation increases the amount of information per spike, the total information available in the spike train is still smaller than in the case of $V_r = -60$ mV. We argue that even if this is so, the amount or type of information about the input available in the decorrelated spike train might be already sufficient for certain sensory based decisions. For example, we computed the squared reconstruction errors, $[(|\mathrm{I1} - \mathrm{Ir}|)/|\mathrm{I1}|]^2$, where Ir is the optimal linear reconstruction of the light intensity input I1, given by applying a Wiener filter to the LGN's output spike train. The errors for both cases $V_r = -60$ mV and -80 mV were 0.06 and 0.10 respectively. The amount of information in the decorrelated spike train is comparable with the one from the cell at $V_r = -60$ mV, even though in the former case the firing rate has been reduced by four times.

4 Conclusion and Discussion

Biophysical properties of LGN cells support the role of temporal decorrelation which improves efficiency of information processing. This enables a plausible feedback control mechanism on a longer time scale when input statistics change.

If the goal of the LGN is to improve coding efficiency, our work places then the following experimental hypothesis to be tested in behaving animals: the resting membrane potential of LGN relay cells and the tonic/burst characteristics of their spike trains should depend on the temporal correlations of the visual stimulus and on the task demands.

Acknowledgements

This work was supported by grants CNPq (Brazil) and NIMH MH019116.

References

[1] Crick F (1984) Function of the thalamic reticular complex: the searchlight hypothesis. Proc. Natl. Acad. Sci. USA 81: 4586–4590.

[2] Dong DW, Atick JJ (1995) Temporal decorrelation: a theory of lagged and nonlagged responses in the lateral geniculate nucleus. Network: Computation in Neural Systems 6: 159–178.

[3] Dong DW, Atick JJ (1995) Statistics of natural time-varying images. Network: Computation in Neural Systems 6: 345–358.

[4] Guido W, Lu SM, Sherman SM (1992) Relative contributions of burst and tonic responses to the receptive field properies of lateral geniculate neurons in the cat. Journal of Neurophysiology 68: 2199–2211.

[5] Harth E, Unnikrishnan KP (1985) Brainstem control of sensory information: A mechanism for perception. Int J of Psychophys 3: 101–119.

[6] Kaplan E, Shapley R (1982) What controls information processing in the LGN? Society for Neuroscience Abstract 8: 405.

[7] Levine MW, Troy JB (1986) The variability of the maintained discharge of cat dorsal lateral geniculate cells. J Physiol (Lond) 375: 219–246.

[8] Lu SM, Guido W, Sherman SM (1992) Effects of membrane voltage on receptive field properties of lateral geniculate neurons in the cat: contributions of the low-threshold Ca^{2+} conductance. Journal of Neurophysiology 68: 2185–2198.

[9] McCormick DA, Huguenard JR (1992) A model of the eletrophysiological properties of thalamocortical relay neurons. Journal of Neurophysiology 68: 1384–1400.

[10] Mukherjee P, Kaplan E (1995) Dynamics of neurons in the cat lateral geniculate nucleus: in vivo electrophysiology and computational modeling. Journal of Neurophysiology 74: 1222–1243.

[11] Reinagel P, Godwin D, Sherman SM, Koch C (1999) Encoding of visual information by LGN bursts. Journal of Neurophysiology 81: 2558–2569.

[12] de Ruyter van Steveninck RR, Lewen GD, Strong SP, Koberle R, Bialek W (1997) Reproducibility and variability in neural spike trains. Science 275: 1805–1808.

[13] Sherman SM, Koch C (1986) The control of retinogeniculate transmission in the mammalian lateral geniculate nucleus. Exp Brain Res 63: 1–20.

[14] Singer W (1977) Control of thalamic transmission by corticofugal and ascending reticular pathways in the visual system. Phys Reviews 57: 386–420.

Wilson A. Truccolo-Filho is a graduate student at the Center for Complex Systems and Brain Sciences at Florida Atlantic University. His main research interests are in the field of theoretical neuroscience and functional specialization and integration in the visual cortex.

Dawei W. Dong is an assistant professor at the Center for Complex Systems and Brain Sciences at Florida Atlantic University. His research goal is to uncover fundamental principles of how the nervous system codes and uses sensory information.